# Determination of the Transition Temperature at Different Cooling Rates and Its Influence on Prediction of Shrinkage and Warpage in Injection Molding Simulation

**Thomas Lucyshyn,[1] Gilbert Knapp,[2] Michael Kipperer,[1] Clemens Holzer[1]**

[1]*Chair of Polymer Processing, Montanuniversitaet Leoben, Otto Gloeckel-Str. 2, 8700 Leoben, Austria*
[2]*PCCL Polymer Competence Center Leoben GmbH, Roseggerstrasse 12, 8700 Leoben, Austria*

Received 21 December 2010; accepted 27 March 2011
DOI 10.1002/app.34591
Published online 11 August 2011 in Wiley Online Library (wileyonlinelibrary.com).

**ABSTRACT:** In injection molding simulation the phase change from melt to solid state is usually simplified by using a so called transition temperature. In the present work, the transition temperatures of several amorphous and semicrystalline polymers were determined using DSC-runs at different cooling rates. The transition temperature was described as a function of cooling rate. The obtained transition temperatures of the semicrystalline polymers were used in injection molding simulations with the commercial software package Autodesk Moldflow Insight 2010 to calculate the shrinkage and warpage of box-shaped test parts. The simulation results were compared with the experimental values of optically measured injection-molded boxes. The results showed a strong influence of the transition temperatures on the simulation results of a 3D model and a very low influence for a 2.5D model. Transition temperatures obtained at higher cooling rates improved the 3D simulation results for several dimensions. © 2011 Wiley Periodicals, Inc. J Appl Polym Sci 123: 1162–1168, 2012

**Key words:** injection molding; differential scanning calorimetry; simulations; thermal properties

## INTRODUCTION

The computer simulation of shrinkage and warpage of injection molded parts is a difficult task. Commercial software packages offer such options, but the accuracy of the results is not always sufficient. Regarding the highly complex material behavior of thermoplastic polymers, it is clear that the correct determination of material data is an important need for the injection molding simulation. Especially a correct modeling of the phase change from melt to solid state is a major challenge. There are numerous research groups investigating the phase change phenomena,[1–3] but because of the complex physics of the phase change of thermoplastic polymers up to now the typical approach in simulation is the rather simple concept of the no-flow or transition temperature, which defines the limit between melt and solid. As soon as the temperature of the polymer is below the transition temperature, it is defined as a solid with zero flow velocity. This temperature can be either determined on a high pressure capillary rheometer, whereas Autodesk Moldflow Insight (AMI) nowadays uses the results of differential scanning calorimetry (DSC) measurements at a cooling rate of 20 K/min.[4] Due to the well known fact that the cooling rate has a strong influence on the DSC curves[5–7] and that much higher cooling rates up to $\sim$ 1000 K/min occur in real injection molding processes, the target of this work was to determine the transition temperatures from DSC curves obtained at different cooling rates using a commercially available DSC measuring device. Common DSC measurement devices offer only limited cooling rates up to 100 K/min. To be able to extrapolate the transition temperature to even higher cooling rates, a mathematical approximation of the transition temperature as a function of the cooling rate should be found. The influence of the varying transition temperatures on the simulation of shrinkage and warpage with AMI was the final aim of these investigations. Whereas published sensitivity studies[4,8] of the transition temperature on simulation results assume a variation of the transition temperature only by arbitrarily changing its value, this work provides a variation of the transition temperature based on measurements performed at different cooling rates.

As reported in literature, there is a difference in simulation results with AMI using 2.5D-models or true 3D-models.[9–11] Therefore the simulations in AMI were also performed using a Dual Domain model (2.5D-model) and a true 3D-model to find out if there is a difference in the sensitivity of these two models to the transition temperature.

In the Dual Domain model (2.5D), triangle elements on the surface of the part model are used.[4] The governing equations for the numerical description of the melt flow are based on the 2.5D Hele-Shaw approach

*Correspondence to:* T. Lucyshyn (thomas.lucyshyn@unileoben.ac.at).

introduced by Hieber and Shen,[12] which is a mixture between finite difference and finite element method. Contrary, the true 3D-model used in AMI uses tetrahedron elements and full 3D Navier Stokes equations which are solved by the finite element method.[4,11]

## EXPERIMENTAL

### Determination of transition temperature

The transition temperature was determined using a commercially available DSC 1 device by Mettler Toledo International Inc. (USA). A small sample of the investigated polymer and a reference sample are put into a temperature controlled furnace chamber (Fig. 1). The furnace is heated to the desired starting temperature and then cooled down at a defined cooling rate. Following the temperature program the heat flow difference between polymer and reference sample to obtain the same temperatures is measured as a function of temperature.

It has to be mentioned that the applied cooling rate is not constant over the whole temperature range, but rather decreases with lower temperatures (according to the decreasing temperature gradient between sample and cooling agent). Figure 2 shows the cooling rate that can be achieved with the DSC 1 device as a function of temperature. In principle, this behavior is similar to the conditions in an injection mold, where the cooling rate also decreases with lower temperatures of the injection molded part.

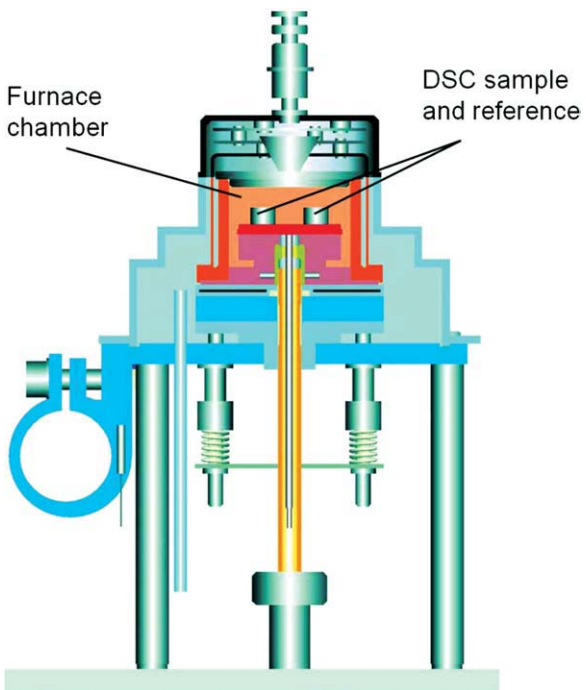


**Figure 1** Mettler Toledo DSC 1 device for determination of the transition temperature.[13] [Color figure can be viewed in the online issue, which is available at www.wileyonlinelibrary.com.]

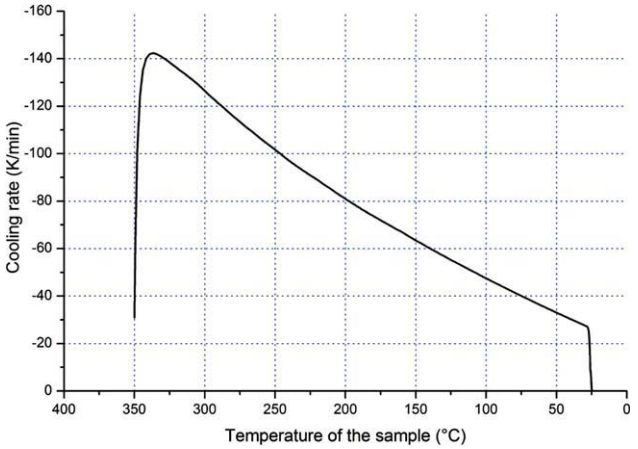


**Figure 2** Cooling rate of the DSC 1 as a function of temperature, measured without polymer sample. [Color figure can be viewed in the online issue, which is available at www.wileyonlinelibrary.com.]

To find out the influence of cooling rate on the transition temperature of different thermoplastic materials, two amorphous and two semicrystalline polymers were investigated. The material grades are summarized in Table I.

The determination of the transition temperatures from the heat flow functions obtained by the DSC-measurements is explained in the following section. For semicrystalline polymers, the transition temperature was obtained at the intersection of the tangents to the heat flow curve in the steep section of the crystallization peak and above it (Fig. 3).

The transition temperatures of the amorphous polymers were defined as the temperatures at the point of inflection of the heat flow curve in the transition range. To find the exact point of inflection, the first derivative of the heat flow curve was plotted as a function of temperature. The maximum value of the first derivative in the glass transition region marks the transition temperature (Fig. 4).

### Injection molding experiments

To be able to compare the simulation results with real parts, test parts were produced on a fully electric injection molding machine (Battenfeld 1000 CD-SE, Austria). The basic part geometry was a box with the dimensions 100 mm × 100 mm × 40 mm (CAD-

**TABLE I**
**Investigated Material Grades**

| Grade name | Supplier | Morphology |
|---|---|---|
| PS 454 C | BASF, Germany | Amorphous |
| ABS Urtal M122 | Polimeri Europa, Italy | Amorphous |
| PP Hostacom BR 735 G | Basell Polyolefins, Netherlands | Semicrystalline |
| PC/PET Stapron E EM 605 | DSM Engineering Plastics, Netherlands | Semicrystalline |

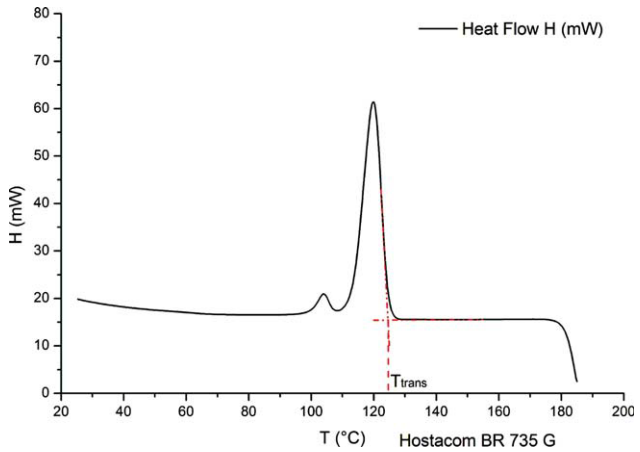


**Figure 3** Heat flow $H$ as a function of temperature $T$ for the determination of the transition temperature of semicrystalline materials (example PP, cooling rate 20 K/min). [Color figure can be viewed in the online issue, which is available at www.wileyonlinelibrary.com.]

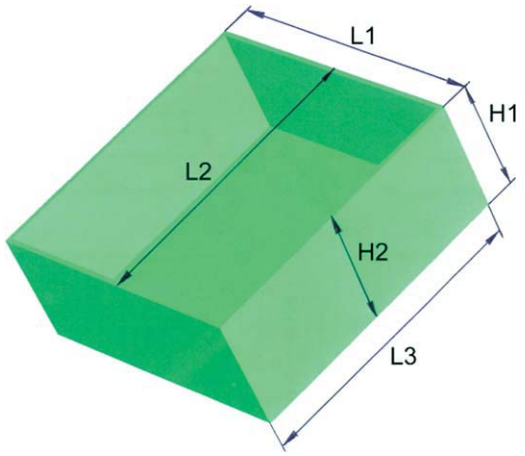


**Figure 5** Model of the box that was used for simulation and injection molding experiments with the chosen dimensions for the comparison of simulation and experiment. [Color figure can be viewed in the online issue, which is available at www.wileyonlinelibrary.com.]

model of the box, Fig. 5). Using different mold inserts, the wall thickness of the bottom and the side walls of the box were different for PP (1 mm) and PC/PET (1.8 mm). The gate is positioned at the center of the box and the mold is equipped with a hot runner. The process settings of the injection molding machine were recorded and used for the simulations (Table II). For each setting, the machine was run in fully automatic mode, and after 30 shots to assure steady state conditions on the machine five parts were produced for the final evaluation.

### Measuring of the injection molded parts

After producing the parts, the complete geometry was measured using an optical 3D-scanner (ATOS II SO from GOM - Gesellschaft fuer optische Messtechnik, Germany) at the Polymer Competence Center Leoben GmbH, Austria (Fig. 6).

The system consists of a projector and two digital cameras with high resolution. The projector generates a strip pattern on the measured part, which is recorded by the two cameras. The measuring principle is similar to the human three-dimensional viewing capability. Using the two photos of the part from two different viewing angles, the evaluation software calculates the three-dimensional shape of the part surface. By attaching reference points to the part, photos from different sides can be overlaid to compose a complete 3D-surface geometry that can be used to compare the real part geometry with the shrinkage and warpage results obtained by simulation. For an easier evaluation, a number of characteristic dimensions of the box were chosen for comparison (Fig. 5): The four side lengths at the rim of box were averaged to the dimension $L1$. The two

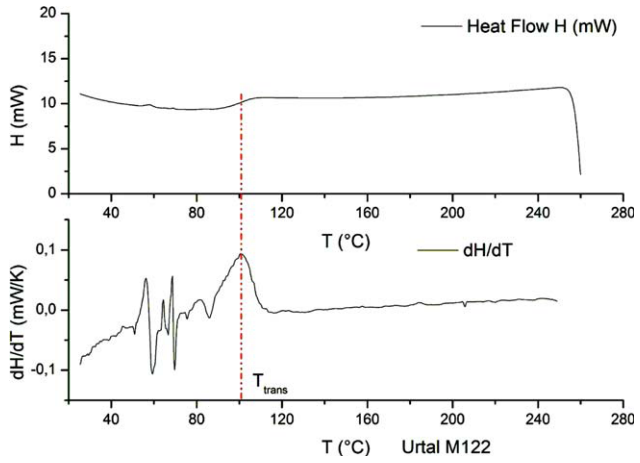


**Figure 4** Heat flow $H$ and first derivative $dH/dT$ of the heat flow as a function of temperature $T$ for the determination of the transition temperature of amorphous polymers (example ABS, cooling rate 20 K/min). [Color figure can be viewed in the online issue, which is available at www.wileyonlinelibrary.com.]

**TABLE II**
**Process Settings of the Injection Molding Experiments and Simulation Runs**

| Parameter | PP Hostacom BR 735 G | PC/PET Stapron E EM 605 |
|---|---|---|
| Melt temperature (°C) | 220 | 255 |
| Mold temperature fixed half (°C) | 40 | 60 |
| Mold temperature moving half (°C) | 30 | 60 |
| Packing pressure (MPa) | 51 | 44 |
| Filling time (s) | 1.9 | 2.4 |
| Packing time (s) | 5 | 8 |
| Cooling time (s) | 25 | 8.4 |
| Mold open time (s) | 7.9 | 4.8 |
| Cycle time (s) | 39.8 | 23.6 |

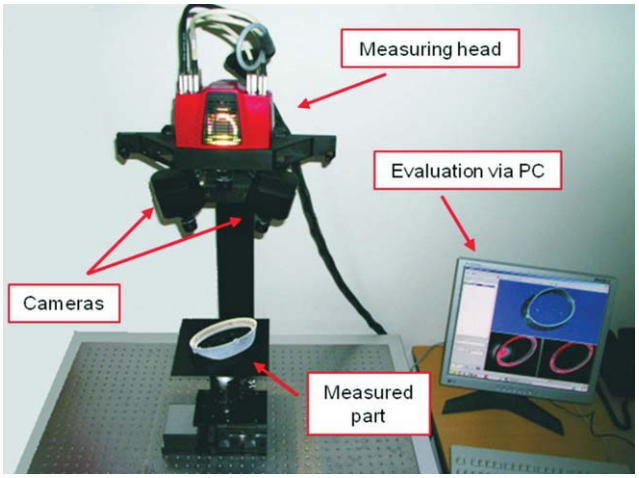


**Figure 6** Optical 3D-scanner ATOS II SO (GOM, Germany) for the measuring of the injection molded parts. [Color figure can be viewed in the online issue, which is available at www.wileyonlinelibrary.com.]

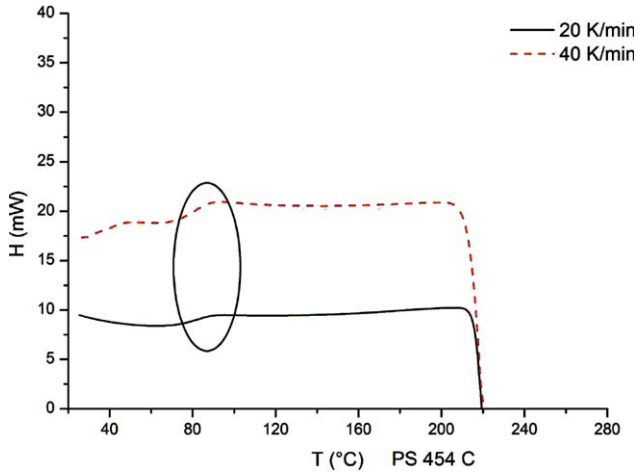


**Figure 7** Heat flow as a function of temperature at two different cooling rates for polystyrene PS 454 C. [Color figure can be viewed in the online issue, which is available at www.wileyonlinelibrary.com.]

distances of opposite side walls at the rim of the box were averaged to the dimension *L*2. The average value of the four lengths at the bottom of the box was defined as the dimension L3. Furthermore, the dimension *H*1 is the mean value of the four heights of the side walls at the corners and finally *H*2 is the average value of the height in the middle of the four sidewalls.

### Simulation with Autodesk Moldflow Insigth 2010 (AMI)

Using the process settings of the injection molding experiments, the test parts were simulated with AMI, including the cooling and runner system. Separate simulations were performed using the transition temperatures obtained from DSC-measurements at different cooling rates. A varying cooling rate over the part geometry, which can occur in reality could not be taken into account in the simulations, as such a functionality was not yet implemented in AMI. Each simulation run was performed with a different transition temperature obtained at a certain cooling rate which was a constant value for the whole geometry. Finally, the calculated deformations of the dimensions *L*1, *L*2, *L*3, *H*1, and *H*2 were evaluated. The deformation is defined as the relative difference between mold cavity and final part dimensions.

## RESULTS AND DISCUSSION

### Transition temperatures at different cooling rates

As the recommended cooling rate for the determination of the transition temperature according to AMI is 20 K/min, this cooling rate was used as a reference. For the investigated amorphous materials, no significant influence of the cooling rate on the transition temperature was observed. Figure 7 shows the heat flow curves of PS 454 C as a function of temperature at cooling rates of 20 K/min and 40 K/min. The transition region (marked with circle) remains almost unchanged.

The results for the second amorphous polymer (ABS Urtal M122) are very similar. As with the polystyrene, there is no remarkable shift in the transition region (Fig. 8).

As a consequence of this findings it can be assumed that the determination of the transition temperature at a standard cooling rate of 20 K/min is sufficient. Therefore no computer simulations were performed with the amorphous polymers.

As expected, the heat flow curves of the investigated semicrystalline polymers showed a significant

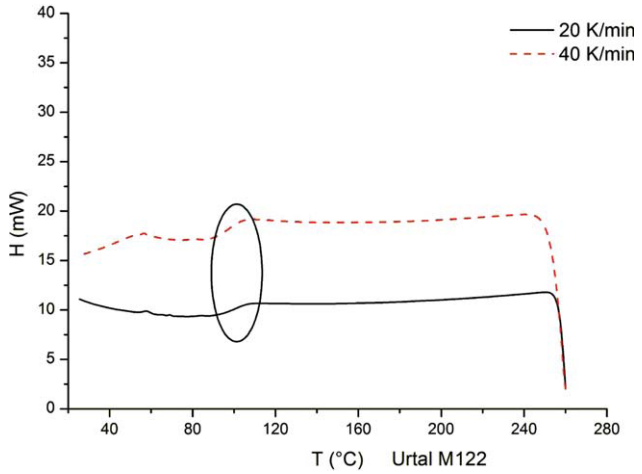


**Figure 8** Heat flow as a function of temperature at two different cooling rates for ABS Urtal M122. [Color figure can be viewed in the online issue, which is available at www.wileyonlinelibrary.com.]

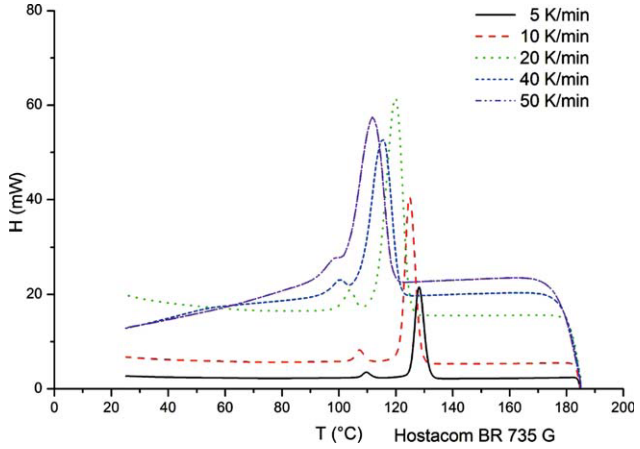


**Figure 9** Heat flow as a function of temperature at different cooling rates for PP Hostacom BR 735 G. [Color figure can be viewed in the online issue, which is available at www.wileyonlinelibrary.com.]

sensitivity to higher cooling rates. This behavior has already been described well in several publications.[5–7] Target of the present research was the determination of the transition temperature as a function of cooling rate with a commercially available testing device. In principle, the maximum cooling rate achievable with the DSC 1 should be 100 K/min. During the investigations it turned out that reasonable results for the investigated materials could only be achieved up to about 70 K/min. Figure 9 shows the heat flow curves of the polypropylene Hostacom BR 735 G as a function of temperature and at different cooling rates (5, 10, 20, 40, and 50 K/min). The shift of the transition temperature to lower temperatures with increasing cooling rates can clearly be seen.

For the PC/PET blend with mainly semicrystalline character Stapron E EM 605 cooling rates up to 70 K/min could be achieved. The heat flow curves at the various cooling rates are illustrated in Figure 10. Again, a significant dependence of the transition region on the cooling rate can be observed.

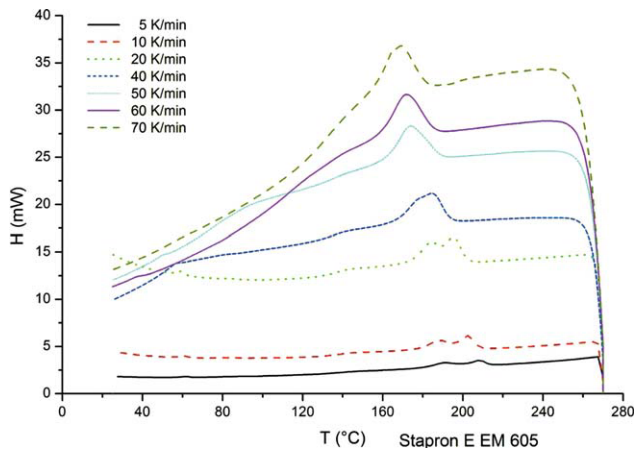


**Figure 10** Heat flow as a function of temperature at different cooling rates for PC/PET Stapron E EM 605. [Color figure can be viewed in the online issue, which is available at www.wileyonlinelibrary.com.]

**TABLE III**
**Material Parameters and Correlation Coefficient $R^2$ for the Approximation of the Transition Temperature as a Function of Cooling Rate**

| Parameter | PP Hostacom BR 735 G | PC/PET Stapron E EM 605 |
|---|---|---|
| $a$ ($\text{min}^b\ \text{K}^{(1-b)}$) | 415.4 | 512.1 |
| $b$ (–) | −0.0148 | −0.0266 |
| Correlation coefficient $R^2$ | 0.983 | 0.94 |

To be able to extrapolate the results to higher cooling rates, a simple mathematical function was found to describe the transition temperature as a function of cooling rate [eq. (1)]:

$$T_{\text{trans}} = a \cdot \left(\frac{\partial T}{\partial t}\right)^b, \tag{1}$$

where $T_{\text{trans}}$ is the transition temperature (K), $\left(\frac{\partial T}{\partial t}\right)$ is the cooling rate (K/min), $a$ is a material parameter ($\text{min}^b\ \text{K}^{(1-b)}$), and $b$ is a material parameter (–).

The material parameters $a$ and $b$ for the two materials are summarized in Table III.

The function shows good agreement with the experimental values of the two materials. The transition temperature as a function of cooling rate for PP Hostacom BR 735 G is shown in Figure 11, and the results for PC/PET Stapron E EM 605 can be seen in Figure 12.

## Shrinkage and warpage simulation results

In the following figures the simulation results performed with the transition temperatures obtained at

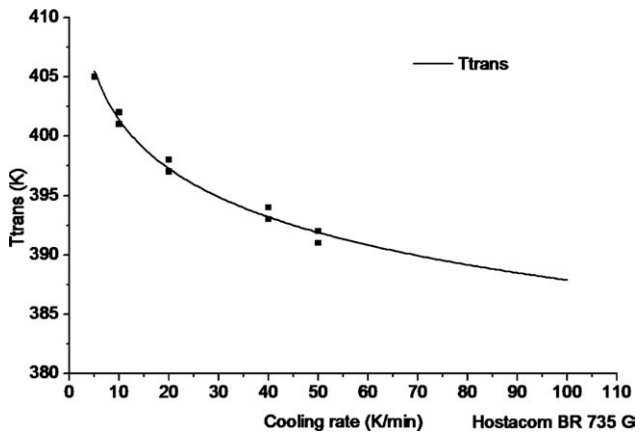


**Figure 11** Transition temperature as a function of cooling rate for PP Hostacom BR 735 G (experimental values and data fit).

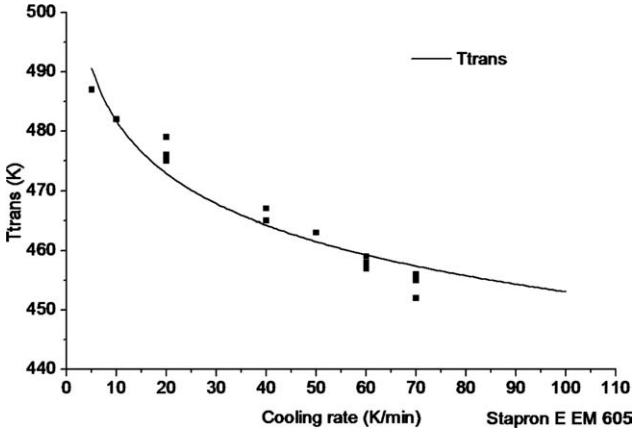


**Figure 12** Transition temperature as a function of cooling rate for PC/PET Stapron E EM 605 (experimental values and data fit).

different cooling rates are compared with the experimental results. The measured part deformations are only drawn into the graphs as reference values, but they were not obtained at different cooling rates. The simulations in AMI were done with 3D as well as 2.5D models. Figure 13 shows the results for the 3D calculation for the PP Hostacom BR 735 G. The predicted shrinkage decreased with transition temperatures obtained at increasing cooling rates. For some dimensions (*L*1 and *L*3) the transition temperatures at higher cooling rates improved the simulation results. The dimension *L*2, which is mainly influenced by warpage (corner effect), could not be predicted well at all for this material. The reason for this is still unclear.

Compared to the 3D model, the influence of the transition temperature on the shrinkage and warpage simulation results for PP Hostacom BR 735 G was much lower in the 2.5D model. The results obtained with the 2.5D model are generally too low compared with the experimental data, especially for

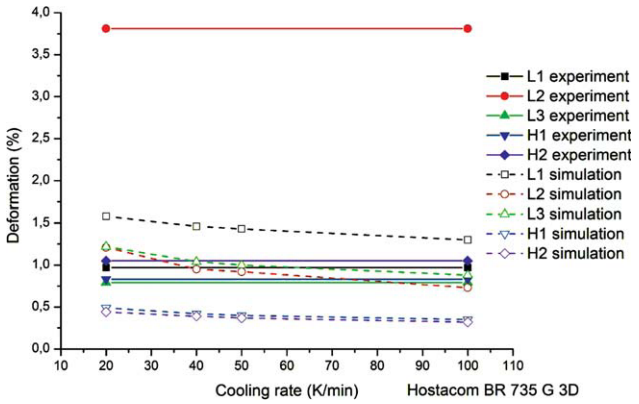


**Figure 13** Shrinkage and warpage simulation results for PP Hostacom BR 735 G (box with 1 mm wall thickness, 3D model). [Color figure can be viewed in the online issue, which is available at www.wileyonlinelibrary.com.]

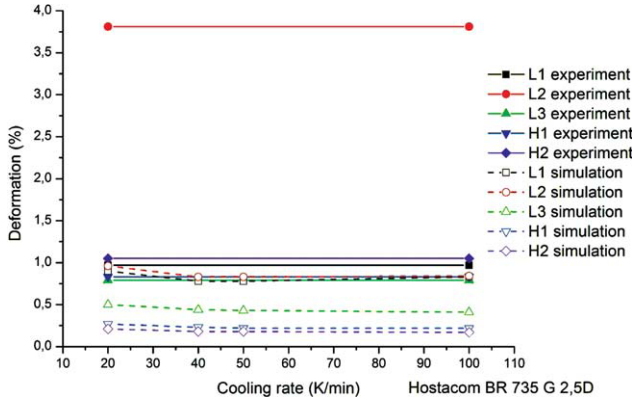


**Figure 14** Shrinkage and warpage simulation results for PP Hostacom BR 735 G (box with 1 mm wall thickness, 2.5D model). [Color figure can be viewed in the online issue, which is available at www.wileyonlinelibrary.com.]

the warpage dominated dimension *L*2, but also for the other dimensions (Fig. 14).

Similar tendencies were found for the PC/PET Stapron E EM 605. Using the 3D model, transition temperatures at higher cooling rates improved the simulation results (Fig. 15). The 2.5D model once again did not show much influence of the transition temperatures on the simulation results (Fig. 16).

## CONCLUSIONS

In this article the influence of cooling rate on the determination of the so called transition temperature with DSC measurement was investigated for two amorphous and two semicrystalline materials. The amorphous polymers hardly showed any sensitivity of the transition temperature to the cooling rate. Contrary, the cooling rate had a strong influence on the transition temperatures of the two semicrystalline polymers. For the latter, a mathematical function was found to describe the dependence of the

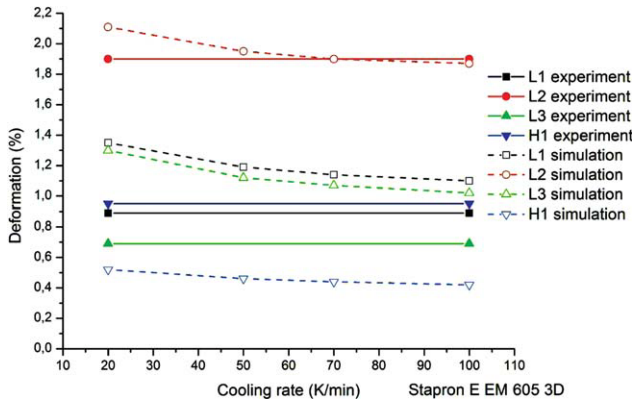


**Figure 15** Shrinkage and warpage simulation results for PC/PET Stapron E EM 605 (box with 1.8 mm wall thickness, 3D model). [Color figure can be viewed in the online issue, which is available at www.wileyonlinelibrary.com.]

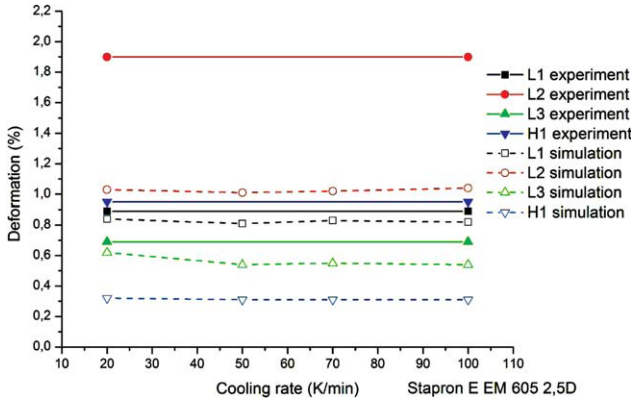


**Figure 16** Shrinkage and warpage simulation results for PC/PET Stapron E EM 605 (box with 1 mm wall thickness, 2.5D model). [Color figure can be viewed in the online issue, which is available at www.wileyonlinelibrary.com.]

transition temperature on the cooling rate to be able to extrapolate to higher rates which are not accessible by standard DSC measurements. Furthermore, this mathematical function can be used for implementation of a cooling rate dependent transition temperature in an injection molding simulation software.

In the next step box-shaped test parts of the two semicrystalline materials were injection molded and subsequently simulated in the commercial injection molding software Autodesk Moldflow Insight 2010 using the experimental process settings. The influence of transition temperatures obtained at different cooling rates on the shrinkage and warpage simulation results was analyzed and the predicted values were compared to the experimental values which had been measured using a 3D optical scanner. The calculations were performed using 3D as well as 2.5D models. The results for the investigated box-shaped parts showed a strong influence of the transition temperatures on simulation results of the 3D model and a very low influence on the 2.5D model. Generally, the simulation results of the 3D models matched better with experimental values. For several dimensions of the investigated test part, the 3D simulation results were improved using transition temperatures at higher cooling rates.

Based on these results further research will be performed additionally taking into account different temperature dependent curves of specific heat at higher cooling rates.

The research work of this paper was performed in cooperation with the Polymer Competence Center Leoben GmbH (PCCL, Austria) within the framework of the COMET-program of the Austrian Ministry of Traffic, Innovation and Technology. The PCCL is funded by the Austrian Government and the State Governments of Styria and Upper Austria.

## References

1. Janeschitz-Kriegl, H. Crystallization Modalities in Polymer Melt Processing—Fundamental Aspects of Structure Formation; Springer: Wien, New York, 2010.
2. Pantani, R.; Coccorullo, I.; Speranza, V.; Titomanlio, G. Prog Polym Sci 2005, 30, 1185.
3. Zuidema, H. Flow Induced Crystallinity of Polymers, Applications to Injection Molding, PhD Thesis; Technical University of Eindhoven, 2000.
4. Kennedy, P. Practical and Scientific Aspects of Injection Molding Simulation, PhD Thesis; Technical University of Eindhoven, 2008.
5. Adamovsky, S.; Minakov, A.; Schick, C. Thermochim Acta 2003, 403, 55.
6. De Santis, F.; Adamovsky, S.; Titomanlio, G.; Schick, C. Macromolecules 2006, 39, 2562.
7. Gradys, A.; Sajkiewicz, P.; Minakov, A. A.; Adamovsky, S.; Schick, C.; Hashimoto, T.; Saijo, K. Mater Sci Eng A 2005, 413–414, 442.
8. Gao, Y.; Turng, L.-S.; Wang, X. Adv Polym Technol 2008, 27, 199.
9. Ni, S. Annu Technical Conference, ANTEC, Conference Proceedings 2009, 4, 2436.
10. Kuppuswamy, V. A.; Spanoudis, S. L.; Petrescu, M.; Nagaraj, B. Technical Conference, ANTEC, Conference Proceedings 2010, 1, 182.
11. Jaworski, M. J.; Yuan, Z. Technical Conference, ANTEC, Conference Proceedings 2003, 1, 642.
12. Hieber, C. A.; Shen, S. F. J Non-Newtonian Fluid Mech 1980, 7, 1.
13. N. N. DSC 1 product information brochure; Mettler-Toledo AG: Schwerzenbach, 2007.